Science Signaling
AAAS

stke.sciencemag.org/cgi/content/full/12/601/eaay0482/DC1

Supplementary Materials for

HIF-independent synthetic lethality between CDK4/6 inhibition and VHL loss across species

Hilary E. Nicholson, Zeshan Tariq, Benjamin E. Housden, Rebecca B. Jennings, Laura A. Stransky, Norbert Perrimon, Sabina Signoretti, William G. Kaelin Jr.*

*Corresponding author. Email: william_kaelin@dfci.harvard.edu

Published 1 October 2019, *Sci. Signal.* **12**, eaay0482 (2019)
DOI: 10.1126/scisignal.aay0482

The PDF file includes:

Other Supplementary Material for this manuscript includes the following:

(available at stke.sciencemag.org/cgi/content/full/12/601/eaay0482/DC1)

Data file S1 (Microsoft Excel format). Results of screen for synthetic lethality with vhl inactivation using dsRNA library in *Drosophila* cells.
Data file S2 (Microsoft Excel format). Results of screen for synthetic lethality with *VHL* inactivation using chemical library in human 786-O and UMRC-2 ccRCC cells.
Data file S3 (Microsoft Excel format). Overlap between genes encoding targets of chemicals that scored in chemical screen and human orthologs of *Drosophila* genes that scored in dsRNA screen.

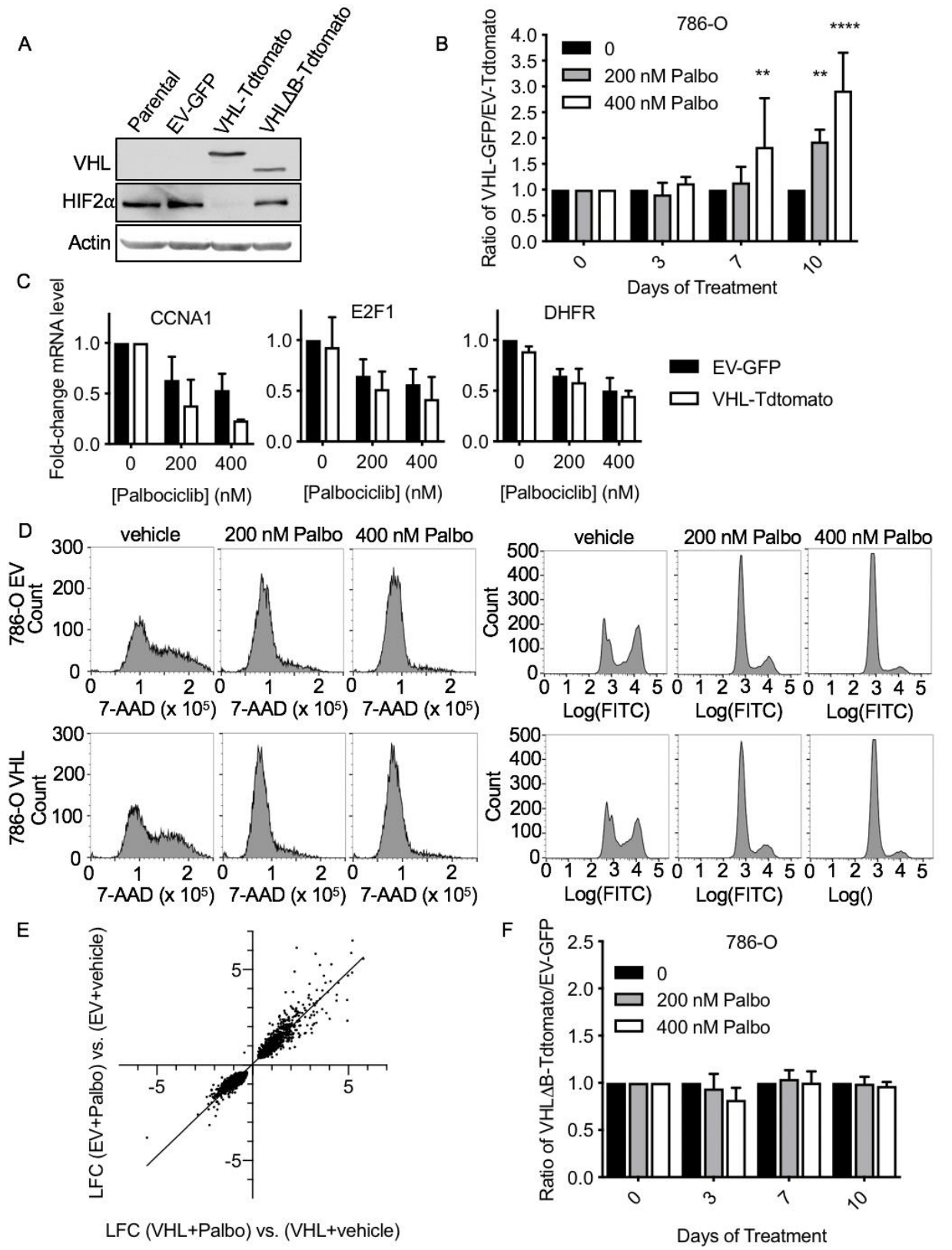
A
Parental
EV-GFP
VHL-Tdtomato
VHLΔB-Tdtomato
VHL
HIF2α
Actin
B
786-O
0
200 nM Palbo
400 nM Palbo
Ratio of VHL-GFP/EV-Tdtomato
Days of Treatment
C
CCNA1
E2F1
DHFR
Fold-change mRNA level
[Palbociclib] (nM)
EV-GFP
VHL-Tdtomato
D
vehicle
200 nM Palbo
400 nM Palbo
786-O EV Count
786-O VHL Count
7-AAD (x 10^5)
Log(FITC)
Log()
E
LFC (EV+Palbo) vs. (EV+vehicle)
LFC (VHL+Palbo) vs. (VHL+vehicle)
F
786-O
Ratio of VHLΔB-Tdtomato/EV-GFP
Days of Treatment

Fig. S1. Control experiments for competition experiments done with isogenic ccRCC cell lines treated with CDK4/6 inhibitors. (**A**) Immunoblot of *VHL*$^{-/-}$ 786-O cells stably infected, where indicated, with a bicistronic lentivirus expressing *VHL* and *Tdtomato* (VHL-Tdtomato), *GFP* alone (EV-GFP), or a *VHL* variant that lacks the β-domain and *Tdtomato* (VHLΔB-Tdtomato). The cells expressing the VHLΔB variant were included for comparative purposes. Blots are representative of 3 experiments. (**B**) Ratio of VHL-GFP-expressing to EV- Tdtomato-expressing 786-O cells that were mixed 1:1 and then treated with 0, 200, or 400 nM palbociclib for the indicated durations. Data are mean ± SD from n=3 independent experiments. (**C**) Relative mRNA expression for *CCNA1*, *E2F1*, and *DHFR* in 786-O cells stably expressing *VHL* or with the empty vector and treated with 0, 200, or 400 nM palbociclib for 48 hours. Data are mean ± SD from n=2 independent experiments. (**D**) Flow cytometry analysis after BrdU incorporation and 7-AAD and BrdU-FITC staining of 786-O cells stably infected with lentivirus expressing VHL (786-O VHL) or the empty vector (786-O EV) and treated 0, 200, or 400 nM palbociclib for 24 hours. Data are representative of 3 experiments. (**E**) Log fold change (LFC) of RNA expression in VHL-Tdtomato and 786-O EV-GFP cells upon treatment with 400 nM Palbociclib or vehicle for 72 hours. (**F**) Ratio of VHLΔB -Tdtomato-expressing to EV-GFP-expressing 786-O cells that were mixed 1:1 and then treated with 0, 200, or 400 nM palbociclib for the indicated durations. Data are mean ± SD from n=3 independent experiments.

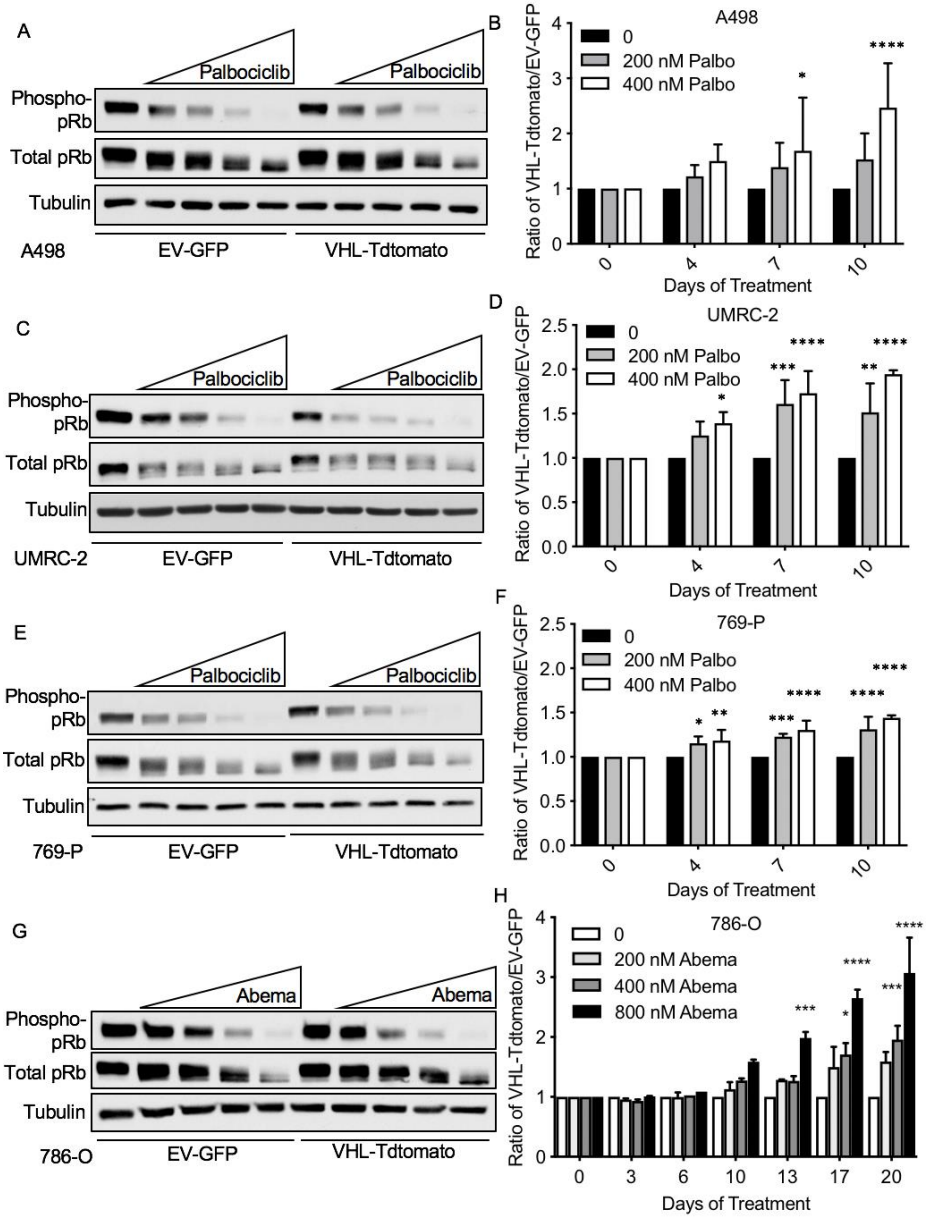

Fig. S2. The CDK4/6 inhibitor palbociclib preferentially inhibits pVHL-deficient cells in various ccRCC cell lines. (**A**) Immunoblots and densitometry analysis of A498 cells stably expressing *VHL* and *Tdtomato* (VHL-Tdtomato) or *GFP* alone (EV-GFP) and treated with 100, 200, 400, or 800 nM palbociclib (as indicated by the triangle) for 24 hours. Blots are representative of 3 experiments. (**B**) Ratio of A498 VHL-Tdtomato cells to EV-GFP cells that were mixed 1:1 and then treated with 0, 200, or 400 nM palbociclib for the indicated durations. Data are mean ± SD of n=5 independent experiments. (**C and D**) As described for (A and B) in UMRC-2 cells. Blots are representative of 3 experiments, and data are mean ± SD of n=3 independent experiments. (**E and F**) As described for (A and B) in 769-P cells. Blots are representative of 3 experiments, and data are mean ± SD of n=3 independent experiments. (**G and H**) As described for (A and B) in 786-O cells. Blots are representative of 3 experiments, and data are mean ± SD of n=2 independent experiments. **P*<0.05, ***P*<0.01, ****P*<0.001, and *****P*<0.0001 by two-way ANOVA tests.

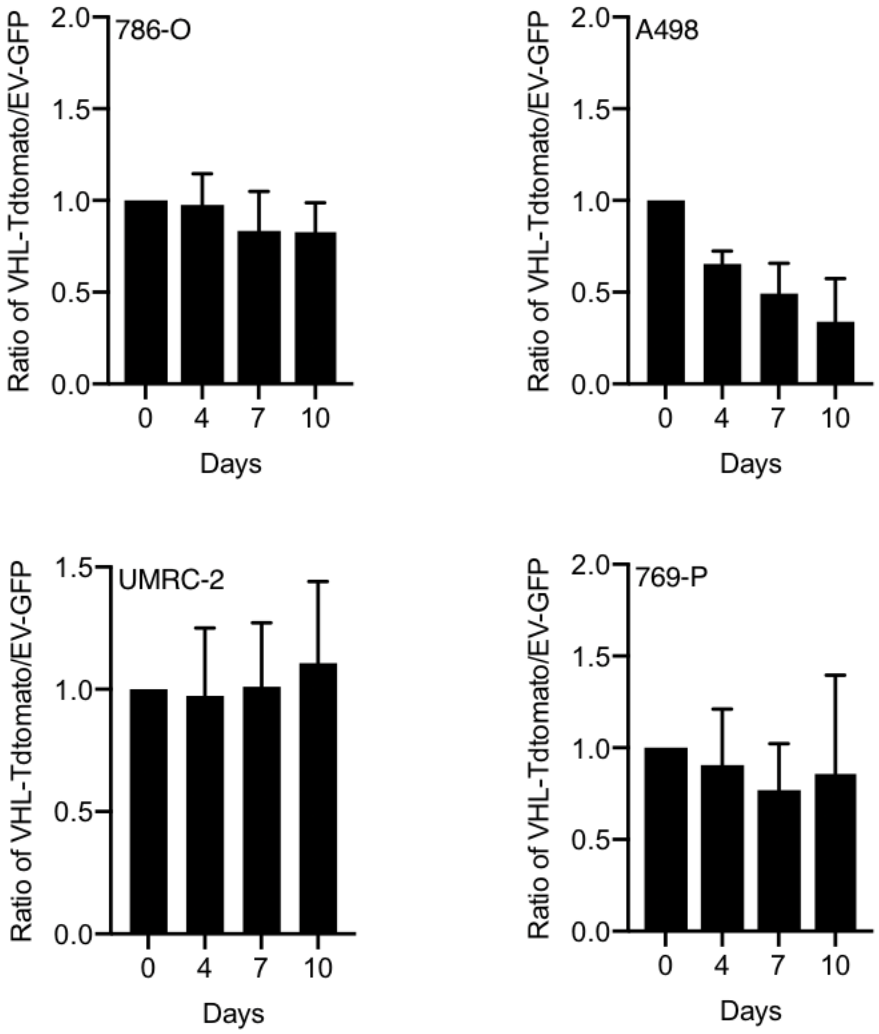

Fig. S3. Changes in proliferation of ccRCC cells after pVHL reconstitution does not account for differential sensitivity to CDK4/6 inhibition. Ratio of 786-O, A498, UMRC-2, and 769-P VHL-Tdtomato cells/EV-GFP cells over time that were mixed 1:1 on Day 0. Data are mean + SD of n=4 independent experiments.

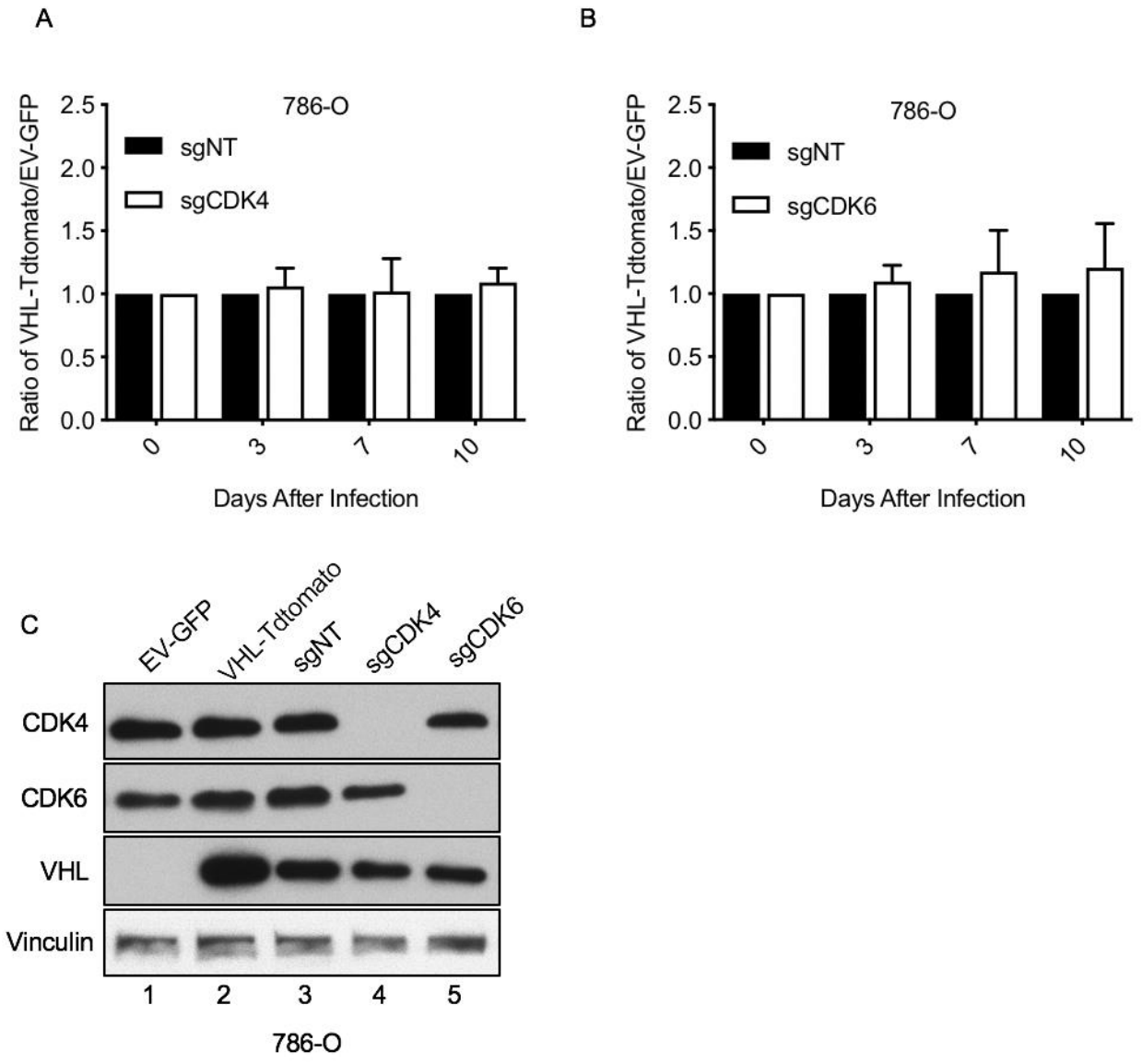

Fig. S4. Individual knockdown of CDK4 or CDK6 does not differentially affect the viability of ccRCC cells based on *VHL* status. (**A and B**) Ratio of VHL-Tdtomato- or EV-GFP-expressing 786-O cells that were mixed 1:1 and then superinfected with a lentivirus expressing the indicated sgRNAs (sgNT = non-targeting control sgRNA). Data are mean ± SD of n=6 (A) or 8 (B) independent experiments. (**C**) Immunoblot of 786-O cells described in (A and B) either prior to (lanes 1 and 2) or 10 days after (lanes 3 to 5) lentiviral infection and mixing. Blot is representative of 3 independent experiments.

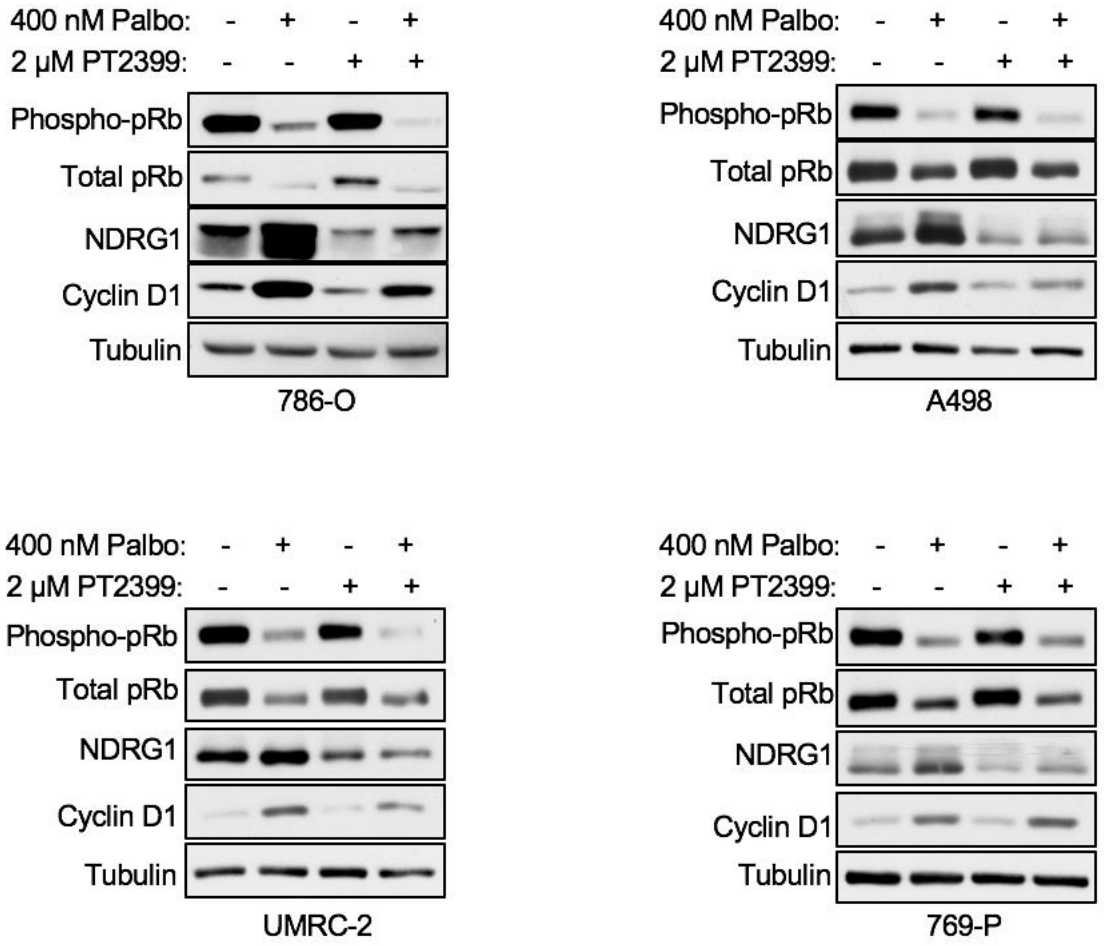

Fig. S5. PT2399 attenuates palbociclib-induced up-regulation of cyclin D1 abundance in HIF-2α–dependent, but not HIF-2α–independent, cell lines. Immunoblot of 786-O, A498, UMRC-2, or 769-P EV-GFP cells treated with 2 μM PT2399, 400 nM Palbociclib, or the combination of both drugs, where indicated for 48 hours. Blots are representative of 3 independent experiments.

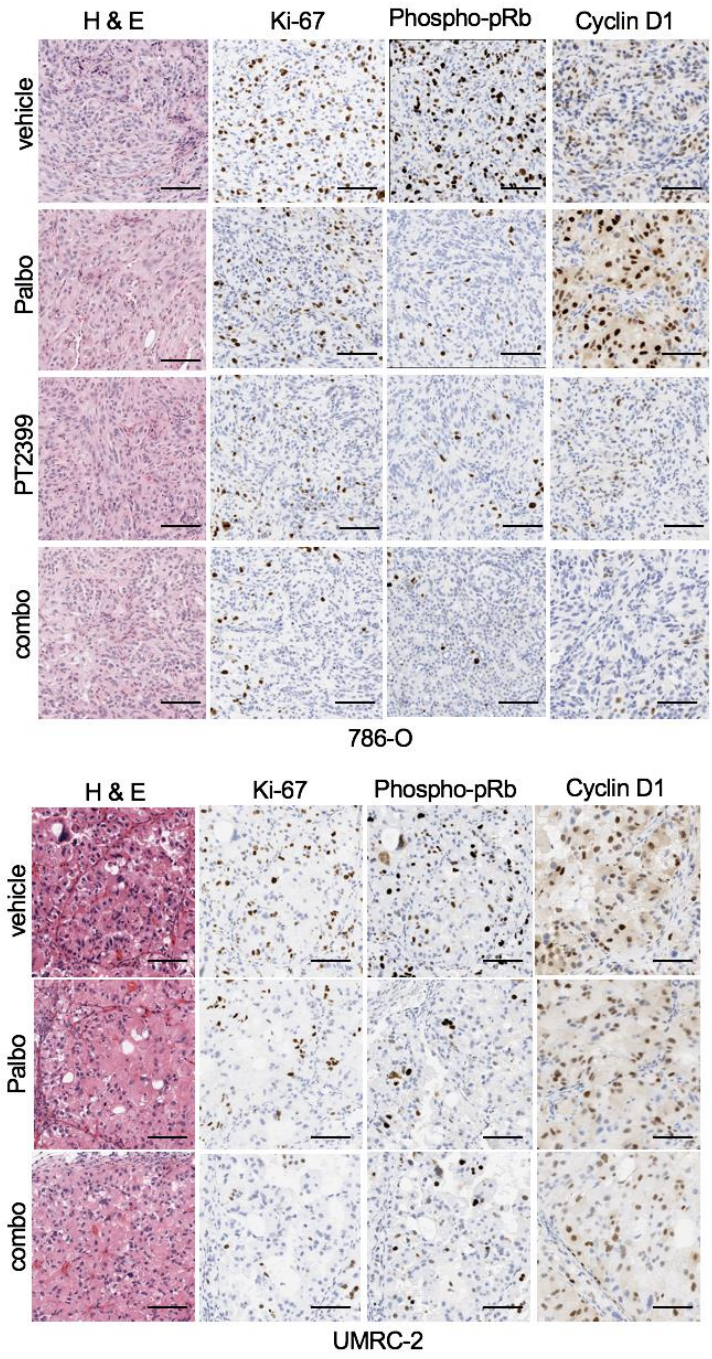

Fig. S6. Effect of palbociclib, PT2399, and their combination on cyclin D1 and phospho-pRb abundance in vivo. Immunohistochemistry of representative 786-O and UMRC-2 orthotopic tumors isolated from mice treated daily for two days by oral gavage with either vehicle, 65 mg/kg palbociclib (Palbo), 20 mg/kg PT2399 (A only), or both (20 mg/kg PT2399 and 65 mg/kg palbociclib; “combo”). Histology images are representative of n=2 mice for each condition. Scale bars, 100 μm.

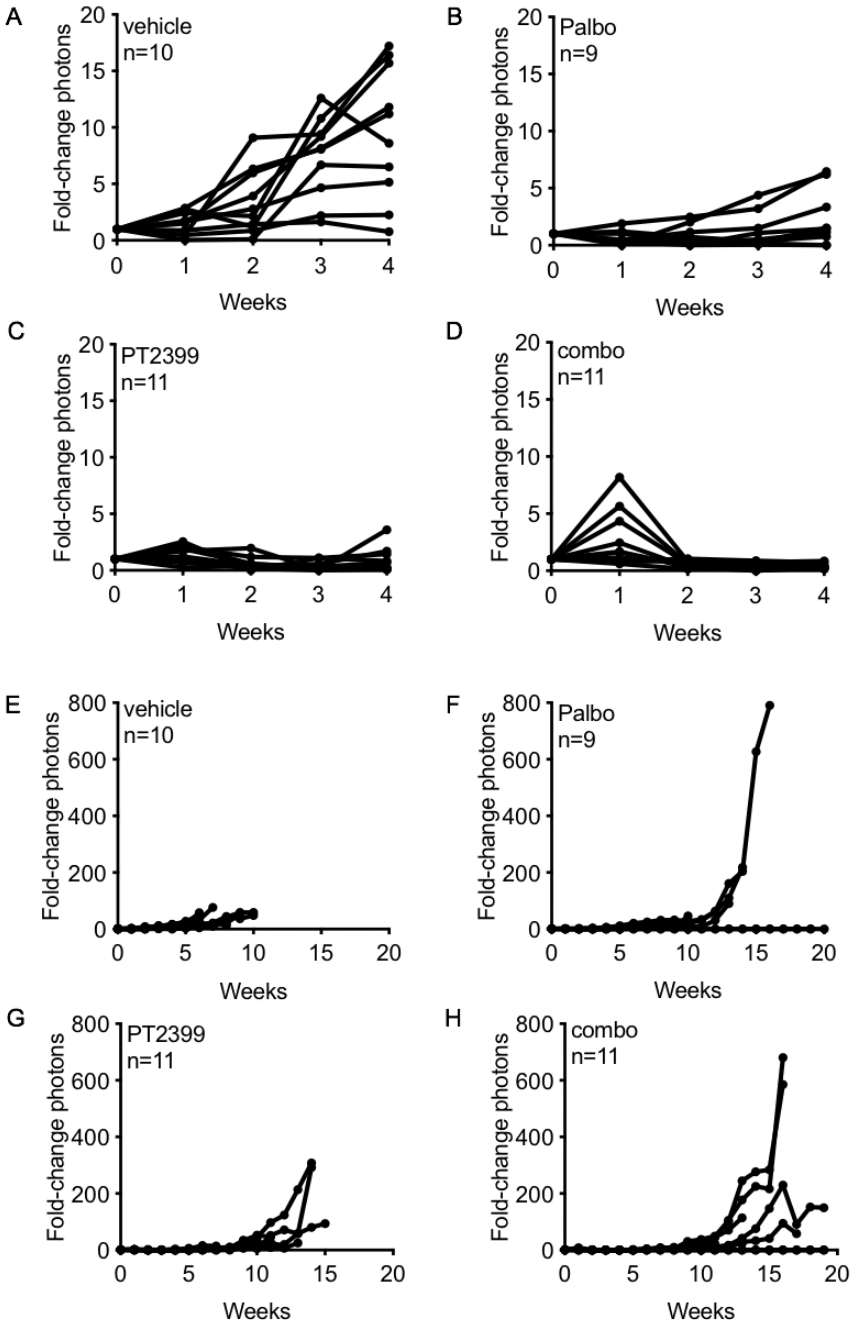

Fig. S7. Growth of ccRCC orthotopic xenografts during treatment with vehicle, palbociclib, PT2399, or their combination. (A to H) Spider plots showing fold-change photons emitted from orthotopic tumors formed by firefly luciferase-expressing 786-O cells as determined by weekly BLI beginning on Day 0 and continuing for 4 weeks (A-D) or up to 20 weeks (E-H) in tumor-bearing mice treated daily for 28 days with vehicle (A and E), 65 mg/kg palbociclib alone (B and F), 20 mg/kg PT2399 alone (C and G), or both (combo; D and H). Each curve represents a different mouse and terminates with the death of that mouse or at 4 and 20 weeks, respectively. At 20 weeks there were 2 mice alive in (F) and 4 mice in (H). The curves for these mice superimpose with the x- axes in these figures.

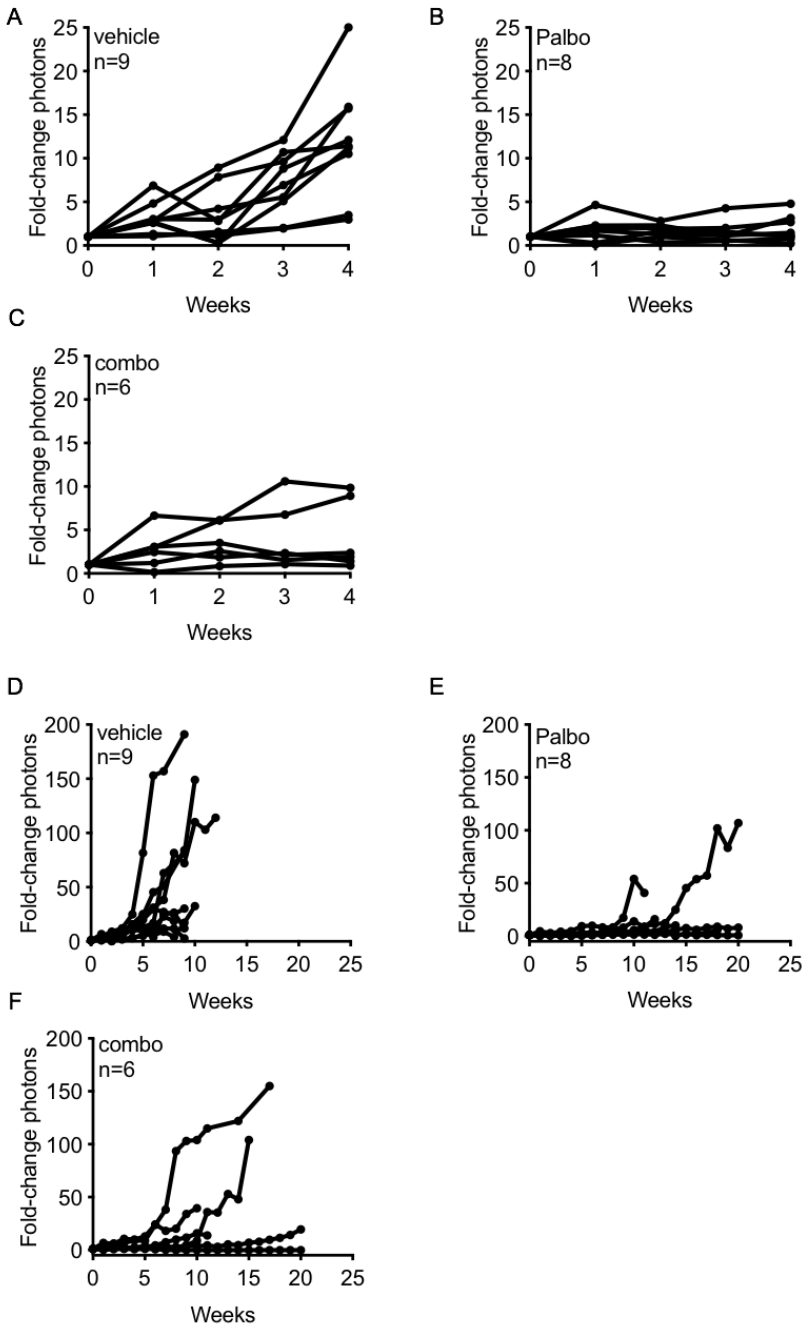

Fig. S8. Growth of HIF-2α inhibition–resistant *VHL*-null ccRCC orthotopic xenografts during treatment with vehicle, palbociclib, or the combination of palbociclib with PT2399. (A to F) Spider plots showing fold-change in photon emission from orthotopic tumors formed by firefly luciferase-expressing UMRC-2 cells as determined by weekly BLI beginning on day 0 and continuing for 4 weeks (A to C) or 20 weeks (D to F) in tumor-bearing mice treated daily for 4 weeks with vehicle (A and D), 65 mg/kg palbociclib alone (B and E), or both 65 mg/kg palbociclib and 20 mg/kg PT2399 (combo; C and F). Each curve represents a different mouse and terminates with the death of that mouse or at 4 and 20 weeks, respectively. At 20 weeks there were 4 mice alive in (D) and 2 mice in (F). The curves for these mice superimpose with the x- axes in these figures.

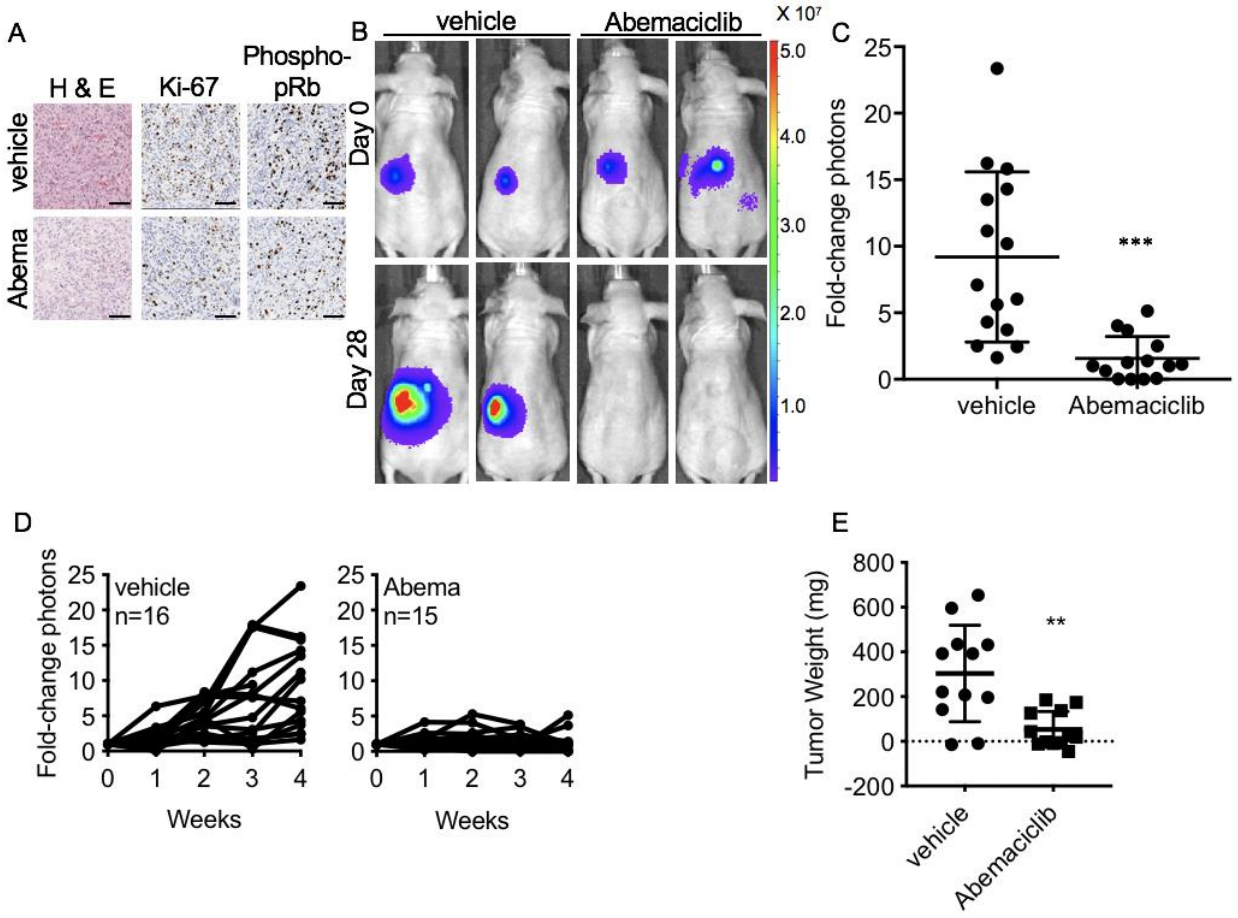

Fig. S9. Antitumor activity of abemaciclib in *VHL*-null ccRCC orthotopic xenografts. (**A**) Immunohistochemistry of 786-O orthotopic tumors treated with vehicle or 60 mg/kg abemaciclib once daily for two days. Histology images are representative of n=2 mice for each condition. Scale bars, 100 μm. (**B**) Representative BLI of orthotopic tumors formed by firefly luciferase-expressing 786-O cells before and after vehicle or 60 mg/kg abemaciclib dosed daily by oral gavage for 28 days (n=15 or 14 mice from two independent experiments, respectively). (**C**) Quantification of BLI for mice described in (B). Photon measures on day 28 were normalized to those on day 0 for each mouse individually (p=0.0004 by Welch's t-test). (**D**) Spider plots showing fold-change in photon emission from tumor-bearing mice described in (B) as determined by weekly BLI over the course of 28 days of treatment with vehicle (left) or abemaciclib (Abema; right). (**E**) Tumor weights from mice described in (B). n=12 mice for vehicle, 11 for abemaciclib; ***P*<0.001 (*P*=0.0020) by Welch's t-test.

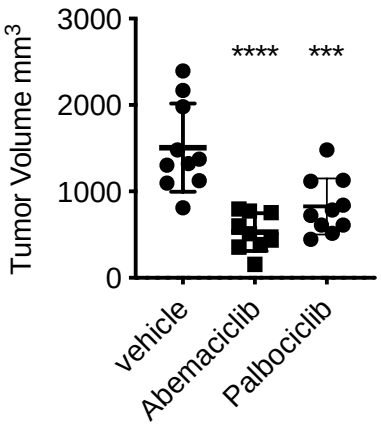

Fig. S10. Antitumor activity of palbociclib and abemaciclib in a ccRCC PDX model. Volume of patient-derived xenograft tumors after 25 days of treatment with vehicle, 75 mg/kg palbociclib daily, or 60 mg/kg abemaciclib twice daily. n=10 mice for vehicle, 9 for abemaciclib, and 10 for palbociclib; ***P<0.001, ***P<0.0001 by one-way ANOVA.

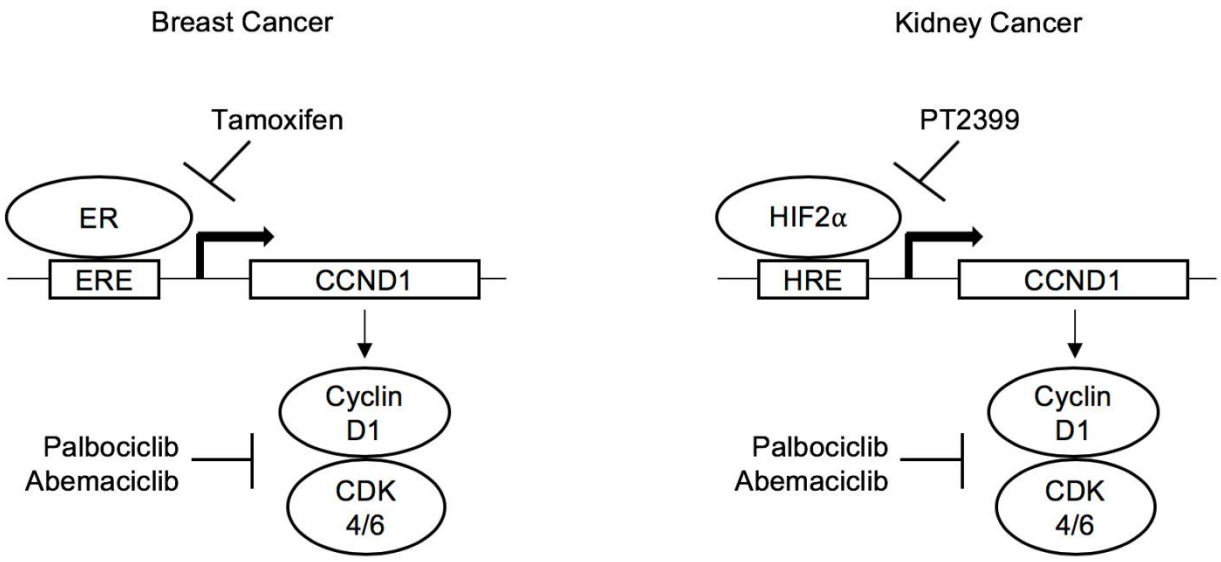

Fig. S11. Schematic of analogous signaling mechanisms in breast cancer and ccRCC. The estrogen receptor (ER) and HIF2α bind to an estrogen response element (ERE) and hypoxia-response element (HRE), respectively, that control the transcription of *CCND1,* which encodes Cyclin D1. In breast cancer ER is a major regulator of *CCND1* and ER antagonists (e.g. tamoxifen) therefore downregulate Cyclin D1. Similarly, HIF2α regulates *CCND1* in ccRCC and HIF2α antagonists (e.g. PT2399) can downregulate Cyclin D1 in HIF2α-dependent ccRCC lines. Adding a CDK4/6 inhibitor enhances the ability of ER antagonists to control breast cancer proliferation, presumably because they both directly or indirectly converge on the activity of CDK4/6. By analogy, adding a CDK4/6 inhibitor might enhance the activity of a HIF2α inhibitor in ccRCC.

Table S1. sgRNA oligonucleotides. The sequences of the sgRNA oligonucleotides used for editing (including BsmBI/Esp3I overhangs) are listed in the table.

sgRNA oligonucleotide target/name	***Sequence***
CDK4 sg1 sense	5'-CACCGGTCCACATATGCAACACCTG-3'
CDK4 sg1 antisense	5'-AAACCAGGTGTTGCATATGTGGACC-3'
CDK4 sg2 sense	5'-CACCGGTCTACATGCTCAAACACCA-3'
CDK4 sg2 antisense	5'-AAACTGGTGTTTGAGCATGTAGACC-3'
CDK6 sg1 sense	5'- CACCGCCAGCAGTACGAATGCGTGG-3'
CDK6 sg1 antisense	5'-AAACCCACGCATTCGTACTGCTGGC-3'
CDK6 sg2 sense	5'-CACCGTGACCAGCAGTACGAATGCG-3'
CDK6 sg2 antisense	5'-AAACCGCATTCGTACTGCTGGTCAC-3'
Non-targeting sgRNA sense	5'-CACCGGGAGGCTAAGCGTCGCAA-3'
Non-targeting sgRNA antisense	5'-AAACTTGCGACGCTTAGCCTCCC-3'
RB1 sense	5'-CACCGCGGTGGCGGCCGTTTTTCGG-3'
RB1 antisense	5'-CCGAAAAACGGCCGCCACCGCGGTG-3'
EPAS1 sense	5'-CACCGTCATGAGGATGAAGTGCA-3'
EPAS1 antisense	5'-AAACTGCACTTCATCCTCATGAC-3'

Table S2. PCR primers. The sequences of the PCR primers used in this study are listed in the table.

Primer target/name	***Sequence***
Drosophila sima forward	5'-TTTGCCATTGAAAACCGACGA-3'
Drosophila sima reverse	5'-CTTGAGGAAAGCGATGGTGAT-3'
Drosophila globin forward	5'-GAAGGTACCGCATAAACATGAACAGCGATGAGG-3'
Drosophila globin reverse	5'-GAAGGTACCGCTGCCTCATCTACTTGGCGTTG-3'
Drosophila LDH forward	5'-GTCTGTTGGCCCAGGTTGCTGAGG-3'
Drosophila LDH reverse	5'-CTGGACATCGGACATGATGTTGGCGGAC-3'
Drosophila CG11652 forward	5'-GTTGGACGTGATCCAACCCAGCAG-3'
Drosophila CG11652 reverse	5'-GATCGTCCAGAGCCGCTGCCTTG-3'
Drosophila act5c forward	5'-GAGCGCAAGTACTGTGTCTGG-3'
Drosophila act5c reverse	5'-GACTCGTCGTACTCCTGCTGG-3'
Human *CCNA1* forward	5'-GCACCCTGCTCGTCACTTG-3'
Human *CCNA1* reverse	5'-CAGCCCCCAATAAAAGATCCA-3'
Human *E2F1* forward	5'-CTTCGTAGCATTGCAGACCC-3'
Human *E2F1* reverse	5'-TATGGTGGCAGAGTCAGTGG-3'
Human *DHFR* forward	5'-GGTCTGGATAGTTGGTGGCA-3'
Human *DHFR* reverse	5'-AACACCTGGGTATTCTGGCA-3'
Human *ACTB* forward	5'-ACCAACTGGGACGACATGGAGAAA-3'
Human *ACTB* reverse	5'-TAGCACAGCCTGGATAGCAACGTA-3'
Human *CCND1* forward	5'-CCGTCCATGCGGAAGATC-3'
Human *CCND1* reverse	5'-ATGGCCAGCGGGAAGAC-3'

Data file S1. Results of screen for synthetic lethality with vhl inactivation using dsRNA library in *Drosophila* cells. This data file contains the list of dsRNAs against *Drosophila* genes, the ID of the specific dsRNA amplicons tested, and the Z-scores for the effects of each dsRNA on S2R+ cells that have (WT) or lack (vhl-null) vhl, the *Drosophila* ortholog of the human *VHL* tumor suppressor gene.

Data file S2. Results of screen for synthetic lethality with *VHL* inactivation using chemical library in human 786-O and UMRC-2 ccRCC cells. This data file contains the map of each small molecule library plate, as well as the Z-scores for the effect of each small molecule at each concentration on cellular fitness (as measured by fluorescence of GFP-expressing cells) of 786-O and UMRC-2 cells that lack functional *VHL* (EV) or that have been reconstituted to express functional *VHL* (VHL).

Data file S3. Overlap between genes encoding targets of chemicals that scored in chemical screen and human orthologs of *Drosophila* genes that scored in dsRNA screen. This data file contains the genes in each portion of the venn diagram in Figure 2D.